ON THE INFLUENCE OF LOW-CYCLE DAMAGE ON FRACTURE TOUGHNESS

K. Kálna*

With heavy section structures working under low cycle, fatigue loading conditions a brittle failure may occur. Thus, the question arises how a repeated high strain loading influences the fracture toughness of the material. It is known [1] that individual materials react differently on low-cycle fatigue loading, depending on their chemical composition, microstructure, heat treatment and other parameters. Three types of materials are to be distinguished depending on whether with increasing number of cycles-N at constant amplitude of plastic strain - ε_{PL} the amplitude of load-P either increases, decreases or remains constant, i.e.: cyclic strain hardening, softening and stable materials respectively.

With cyclic strain-unstable materials, representing the majority, most pronounced changes in material behaviour occur during the first and/or the first ten of loading cycles. That state, when a material behaves as a strain-stable one, being defined as saturated. Further intense changes in material properties occur during the final phase of fatigue life when the relative fatigue life N/N_F approaches one (N_F = number of cycles to complete failure). From a practical point of view the second phase i.e. the saturated state is most important due to the fact that real constructions are being designed for that service state.

MATERIALS AND TEST SPECIMENS

In our experiments, for the study of low-cycle fatigue influence on the materials resistance to brittle fracture initiation, the 20ChMA steel, used for primary circuit tubes of PW reactors, was chosen. The chemical composition of the steel according to both heat and plate analyses is given in Table 1. The basic mechanical characteristics are given in Table 2.

These plates were oxygen cut to blocks from which test specimens oriented perpendicularly to the rolling direction were machined. The following test specimen sets were prepared:

- tensile bars of 10 mm in dia,
- Charpy-V notch toughness test specimens,
- K_{IC} test specimens of 30 x 60 mm and 40 x 20 mm cross-section;
- round bars of 25 mm dia. and square bars of 20 x 40 mm cross-section for low cycle fatigue tests.

Some square bars were pre-fatigued to different N/N_F values and then used for machining the K_{IC} specimens of 20 x 40 mm in cross-section (for the sketch see Figure 1).

*Welding Research Institute, Bratislava, Czechoslovakia.

LOW-CYCLE FATIGUE INFLUENCE ON THE MATERIAL

The ε_{PL}-N dependence for the 20ChMA steel is shown in Figure 2. Fatigue tests were performed using a Schenck-Hydropulse PLX 60 testing machine at controlled plastic strain and with a triangle shape of loading cycle. In Figure 2 points corresponding with the start of fatigue crack extension - N_I, as well as with complete rupture - N_F - are plotted (crosses and round points). For the low cycle fatigue life of the 20ChMA steel the following equation was derived from the test results:

$$\varepsilon_{PL} \cdot N_F^{0.511} = 0.195$$

which corresponds very well with published data.

Test results obtained on prismatic test specimens are plotted in the diagram in Figure 2, as well (see square points). The line joining these points is of slightly smaller slope than that corresponding with round test specimens showing differences in N_F values at higher plastic strain values. Generally, however, results of both test specimen types are in a good agreement. Also in Figure 2 are plotted points (triangles) corresponding to different pre-fatigue influence on subsequent K_{IC} test specimens. Comparing the given state with the obtained low cycle fatigue life line the N/N_F values given in Table 3 were obtained.

The 20ChMA steel represents a cyclic strain-softening material, i.e. its cyclic stress-strain curve σ-ε lies lower than the static one and its cyclic yield point is lower than the static one as well.

TESTING METHODS

The fatigue pre-cracking of K_{IC} test specimens was performed at 20°C keeping K_F = 44 MPa·m$^{1/2}$ at the beginning and K_F = 26 to 28 MPa·m$^{1/2}$ at the end of pre-cracking, thus in accordance with the standards CSN 42 0347, ASTM E 399-74 respectively.

The K_{IC}, COD, J_{IC} tests respectively were performed using an Instron 100kN testing machine equipped with additional gauge and X-Y recorder for plotting load versus load point displacement. Cooling baths consisting of alcohol with solid CO_2 and alcohol with liquid nitrogen were used for testing to 198 K and 153 K respectively. The bath's temperature was controlled by laboratory thermometers. The loading rate was chosen to meet the following values:

$$\dot{K} = \frac{dK}{d\tau} = (1.7 \div 2.4) \text{MPa} \cdot \text{m}^{1/2}\ \text{s}^{-1}$$

Two records were plotted simultaneously in individual tests:

load - notch opening displacement ... P-V
load - load point displacement ... P-f

The elastic-plastic fracture toughness - J_{IC} was determined from P - f diagrams using the calculation procedure recommended in [3]. The provisional J_Q value was calculated according to the relation:

$$J_Q = \frac{2A}{b\,B} \tag{1}$$

where: A is the total area under the load - load point displacement diagram up to an instability point. b = (W - a) is the remaining ligament of the specimen.

The validity of J_{IC} values was checked according to the relation:

$$a,\ b,\ B \geq 25\ \frac{J_Q}{\sigma_{flow}} \tag{2}$$

where $\sigma_{flow} = 1/2(\sigma_Y + \sigma_{UTS})$

σ_Y = 0.2% offset yield strength

σ_{UTS} - ultimate tensile strength

At the so called P_{max} approach, i.e. where for the area under the load - load point displacement diagram the P_{max} load is considered, the validity of J_{IC} values was checked according to the relation:

$$M_{max} - 0.3\ Bb^2 \tag{3}$$

where: M_{max} is the maximum applied bending moment at crack location.

Those J_{IC} values were considered as valid ones meeting the conditions of either (2) or (3) relations.

TEST RESULTS

The temperature dependence of J_{IC} was linearized in half logarithmic coordinates

$$\log J_{IC} - \frac{1}{T}$$

Figure 3 shows the temperature dependence of the elastic-plastic fracture toughness - J_{IC}. Those values were considered as not valid corresponding with tests at which subcritical crack extension took place. Regression lines were determined from the valid J_{IC} values and plotted together with the scatter band for about 70% probability.

THE EFFECT OF LOW CYCLE FATIGUE ON MATERIAL'S RESISTANCE TO BRITTLE FRACTURE INITIATION

Nowadays, the J_{IC} fracture toughness parameter is considered as a most appropriate characteristic of material's resistance to brittle fracture initiation in elastic-plastic loading conditions. This parameter will be applied to judgement of low cycle fatigue influence on materials used in our experiments, too.

The test results are presented in Figures 4 to 7. The temperature dependence of J_{IC} is shown in Figure 4. It follows from the diagram that the low cycle fatigue effect applied in the range of relative fatigue life N/N_F - 0.3 to 0.5 improves the fracture toughness of the material in elastic-plastic loading conditions. For a better judgement of this phenomenon it is important to consider whether the increase of J_{IC} values was caused by the hardening effect - i.e. by the increase of load - P_c, or by the softening effect - i.e. by the increase of strain (load point displacement - f, or COD).

Instead of comparing individual P-f diagrams let us analyze the δ_c values corresponding with individual states of low cycle fatigue effects (ε_0, ε_1, ε_2, ε_3). The temperature dependence of δ_c is plotted in Figure 5, which shows that it is of similar character to that of J_{IC}, i.e. that the increase in J_{IC} values was caused by the cyclic strain-softening of the material, by an increase of its strainability, and this means that low cycle fatigue favourably affects the material's fracture toughness. The fractographic examination of test specimens indicated that an initiated crack had propagated firstly aslant, and then came back to the fracture plane again. The slope angle of the fracture surface depends on the degree of low cycle pre-fatigue effect. In specimens unaffected by low cycle this slope angle made up to 5°, while in specimens influenced by low cycle fatigue it made 30 to 45°.

Metallographic examinations of the material in the vicinity of the crack tip revealed that fracture initiation was being accompanied by branching of the crack, which was evident on fracture surfaces, as well. This branching can be observed on specimens both affected and unaffected by low cycle pre-fatigue.

With the aim of explaining the mechanism of the low cycle fatigue effect on fracture toughness behaviour of a material, the dependences of J_{IC} and δ_c on relative low cycle fatigue life N/N_F - considered as an index of material's damage by low cycle fatigue - were plotted into diagrams in Figures 6 and 7 respectively (using data derived from Figures 4 and 5). Two testing temperatures i.e. 210 K and 173 K were chosen because at these temperatures the majority of test results were available. It is evident again, that both J_{IC} and δ_c parameters show a similar character of the dependence on N/N_F . At lower N/N_F values a pronounced increase in J_{IC} values takes place, being slight only at higher N/N_F values, and - according to [2] at $N/N_F \to 1$ a steep decrease in J_{IC} values is observed. Beside the N/N_F value, the change in J_{IC} value also depends on the extent of plastic strain - ε_{PL}. (See the lines for different ε_{PL} values.) Thus, any change in material's fracture toughness cannot be expressed as a change in relative fatigue life N/N_F only. It depends on the value of plastic strain applied and, probably, on testing temperature, holding time at loading and other factors as well.

From a practical point of view it is important to state that with the 20ChMA steel no decrease in fracture toughness due to a previous low cycle fatigue effect takes place up to the fatigue life $N/N_F = 0.5$.

REFERENCES

1. MANSON, S. S., Fatigue, Proc. SESA, 22, 1965, 193.
2. SERENSEN, S. V. and MACHUTOV, N. A., "Brittle Fracture Resistance of Mild Steel After Prior Low Cycle Fatigue Damage", Marianské Lázně, October, 1970.

3. LANDES, J. D. and BEGLEY, J. A., "Test Results from J - Integral Studies - An Attempt to Establish a J_{IC} Testing Procedure", WRL SP 73-FMPWR-P3, October 1973.

Table 1 Chemical Composition of the 20ChMA Steel/in wt%/

C	Mn	Si	P	S	Cr	Ni	Mo	Cu	Al
0.19 0.20	0.55 0.59	0.28 0.34	0.020 0.022	0.009 0.014	0.82 0.90	0.04 0.13	0.12 0.13	0.09	0.040

Table 2 Basic Mechanical Properties of the 80 mm Thick Plate

σ_Y MPa	σ_{UTS} MPa	Elongation %	Reduction of area %	Charpy V notch toughness $J.cm^{-2}$	T_T^{50} °C	T_T^{PL} °C
460	626	22	66	160	-60	-0

T_T^{50} - transition temperature for the Charpy-V specific energy criterion RV = 50J.cm^{-2}

T_T^{PL} - transition temperature for the criterion of 50% crystallinity in fracture surface appearance

Table 3 The Parameters of Pre-Fatigue Influence of Specimens

Δ	ε_{PL}	N_F	N	N/N_F
1	0.005	1350	400	0.30
2	0.005	1350	600	0.44
3	0.008	540	250	0.46

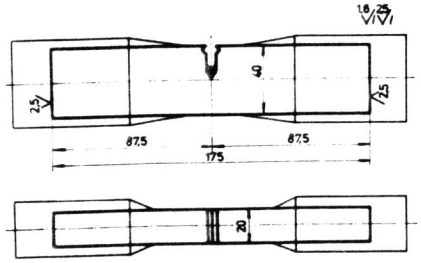

Figure 1 Location of K_{IC} Test Specimen in the Specimen for Low Cycle Fatigue Testing

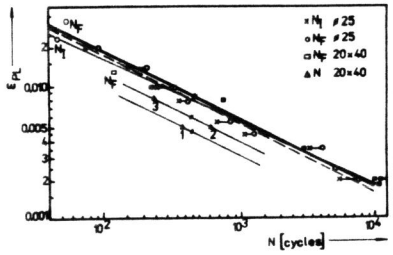

Figure 2 Dependence of Plastic Strain Amplitude ε_{PL} on Cycle Number N

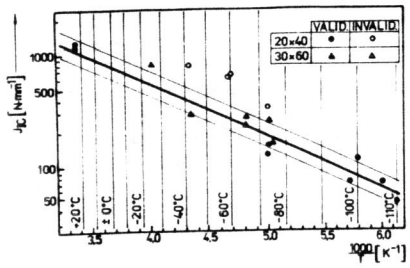

Figure 3 Temperature Dependence of Elastic-Plastic Fracture Toughness - J_{IC}

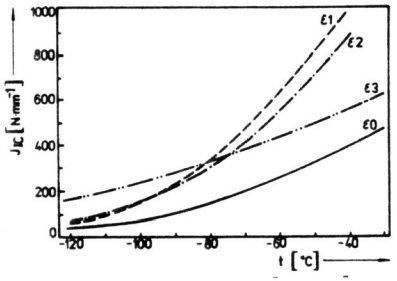

Figure 4 Temperature Dependences of J_{IC} at Different Degrees of Low Cycle Pre-Fatigue Effect

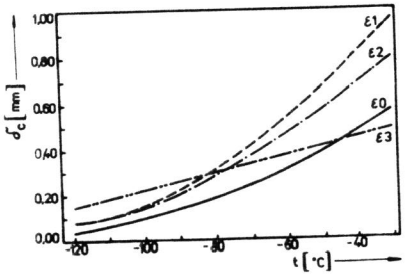

Figure 5 Temperature Dependences of δ_c at Different Degrees of Low Cycle Pre-Fatigue Effect

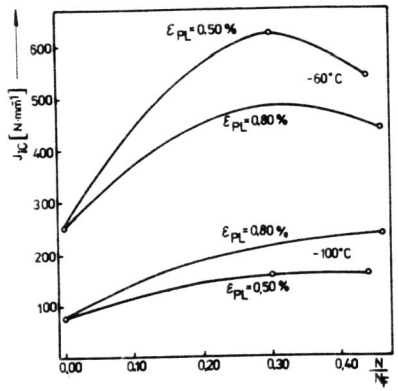

Figure 6 Dependence of J_{IC} on Relative Low Cycle Fatigue Life Values

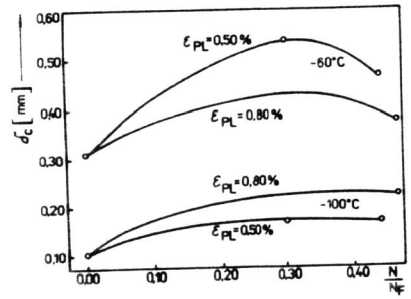

Figure 7 Dependences of δ_c on Relative Low Cycle Fatigue Life Values